JSES International 6 (2022) 297–304

Contents lists available at ScienceDirect

JSES International

journal homepage: www.jsesinternational.org

Can magnetic resonance imaging accurately and reliably measure humeral cortical thickness?

Peter N. Chalmers, MD[a], Garrett V. Christensen, MD[a], Hiroaki Ishikawa, PT, PhD[a,*], Heath B. Henninger, PhD[a], Eugene G. Kholmovski, PhD[b], Megan Mills, MD[b], Robert Z. Tashjian, MD[a]

[a]Department of Orthopaedic Surgery, University of Utah, Salt Lake City, UT, USA
[b]Department of Radiology and Imaging Sciences, University of Utah, Salt Lake City, UT, USA

ARTICLE INFO

Keywords:
Magnetic resonance imaging
Ultra-short time-echo
Computed tomography
Osteoporosis
Cortical thickness

Level of evidence: Basic Science Study; Anatomy; Imaging

Background: Historically, imaging osseous detail in three dimensions required a computed tomography (CT) scan with ionizing radiation that poorly visualizes the soft tissues. The purpose of this study was to determine the accuracy and reliability of ultrashort echo time (UTE) magnetic resonance imaging (MRI) in measuring humeral cortical thickness and cancellous density as compared with CT.

Methods: This was a comparative radiographic study in nine cadavers, each of which underwent CT and UTE MRI. On images aligned to the center of the humeral shaft, anterior, posterior, medial, and lateral humeral cortical thickness was measured 5, 10, and 15 cm distal to the top of the head. Cancellous density was measured as signal within a 1-cm diameter region of interest in the center of the head, the subtuberosity head, the subarticular head, and the subarticular glenoid vault. Glenoid cortical thickness was measured at the center of the glenoid. Cortical measurements were compared using mean differences and 95% confidence intervals, paired Student's t-tests, and intraclass correlation coefficients (ICCs). We compared cancellous measurements using Pearson's correlation coefficients. For all measurements, we calculated interobserver and intraobserver reliability using ICCs with 0.75 as the lower limit for acceptability.

Results: With regard to accuracy, for humeral cortical thickness measurements, there were no significant differences between MRI and CT measures, and ICCs were >0.75. The glenoid cortical thickness ICC was <0.75. There was no significant correlation between the cancellous signal on MRI and on CT in any region. For both MRI and CT, interobserver reliability and intraobserver reliability were acceptable (ie, >0.75) for almost all humeral cortical thickness measures.

Conclusion: UTE MRI can reliably and accurately measure humeral cortical thickness, but cannot accurately measure cancellous density or accurately and reliably measure glenoid cortical thickness.

Assessing bone quality is a critical evaluation before shoulder surgery. Osteoporosis has been demonstrated to be a risk factor for complications in a variety of shoulder procedures.[4,5,15,17,21,30,37] Historically, assessment of bone quality has relied on dual-energy x-ray absorptiometry (DEXA),[1] which has multiple drawbacks. First, DEXA subjects patients to radiation. Second, this scan is not a standard orthopedic evaluation and is thus an additional test that is inconvenient for patients and surgeons. Third, this test provides no information specific to the shoulder as it assesses hip and spine bone density to provide only a global assessment of bone density. Finally, multiple studies have demonstrated that DEXA incompletely assesses fracture risk and bone quality.[20,34] These factors of inconvenience, nonspecificity to the shoulder, and incomplete assessment of bone quality limit the utility of DEXA.

Computed tomography (CT) can reliably measure proximal humeral cortical thickness, which correlates with bone mineral density and can be used to rule out osteoporosis.[23] This imaging is preferable to DEXA as it is specific to the joint, but exposes patients to significantly more ionizing radiation. However, although CT provides excellent visualization of osseous detail, it provides poor

Because this study only involved cadaveric tissue, it did not require institutional review board approval.

The work for this manuscript was performed at the University of Utah in Salt Lake City, UT.

Each author certifies that his or her institution approved the human protocol for this investigation that all investigations were conducted in conformity with ethical principles of research and that informed consent for participation in the study was obtained.

*Corresponding author: Hiroaki Ishikawa, PT, PhD, Department of Orthopaedic Surgery, 590 Wakara Way, Salt Lake City, UT 84108, USA.
E-mail address: ishihiro0211@yahoo.co.jp (H. Ishikawa).

https://doi.org/10.1016/j.jseint.2021.10.010

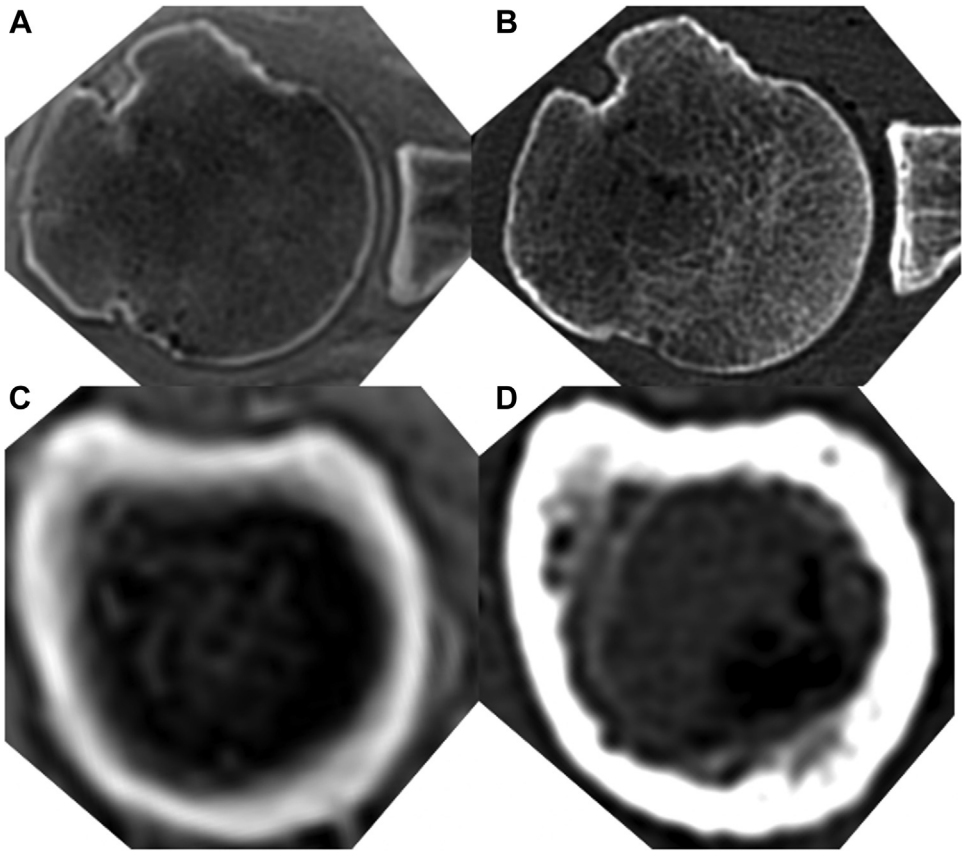

Figure 1 Representative axial images in ultrashort echo time magnetic resonance imaging (UTE MRI) (**A** and **C**) and computed tomography (CT) (**B** and **D**) in the same cadaver at the *Center* of the head (**A** and **B**) and 10 cm distal to the *Top* of the head (**C** and **D**).

visualization of soft tissues, such as the rotator cuff tendons, labrum, and glenohumeral ligaments.[9] As a result, CT is not an ideal preoperative imaging modality before a rotator cuff repair, arthroscopic labral repair, or anatomic shoulder arthroplasty.

Magnetic resonance imaging (MRI) provides excellent soft-tissue detail and can diagnose labral tears and rotator cuff tears with excellent sensitivity and specificity.[14,16,24,26,33] Historically, MRI has provided poor osseous detail in comparison with CT.[6] However, the ultrashort echo time (UTE) MRI sequence[13,34,38] has recently been demonstrated to provide osseous detail sufficient to produce auto-segmented three-dimensional reconstructions that provide equivalent measurements of glenoid bone loss to CT in the setting of glenohumeral instability.[18] UTE MRI, in complement with traditional MRI sequences, may provide the ideal preoperative imaging set for the shoulder as it has no ionizing radiation and excellent resolution of osseous and soft-tissue detail (Fig. 1). However, it remains unclear whether this imaging modality provides sufficient osseous detail to allow assessment of bone quality.

Therefore, the purpose of this study was to determine the accuracy and intraobserver and interobserver reliability of UTE MRI in measurement of humeral cortical thickness, glenoid cortical thickness, and cancellous density as compared with CT.

Materials and methods

Imaging protocol

This is a prospective, cadaveric, controlled, comparative radiographic study. Cadavers from our laboratory underwent both CT and MRI, where both scans were obtained with specimens in a supine anatomic position. The imaging field-of-view included the entirety of the cadaver shoulder for both modalities. CT scans were obtained using a SOMATOM Definition Flash (Siemens, Erlangen, Germany), acquired with a 120 kV tube voltage, 0.6 pitch, 60 mAs tube current, 1.0 mm slice thickness, and 512 x 512 matrix (voxel size = 0.5 x 0.5 × 1.0 mm). MRI studies were performed on the 3 Tesla Prisma (Siemens, Erlangen, Germany) scanner using the head coil. UTE MRI scans were acquired with isotropic spatial resolution (voxel size = 0.7 x 0.7 × 0.7 mm). The scan parameters were echo time (TE) = 0.07 ms, repetition time = 3.64 ms, and flip angle = 6°. The scan time was 3 minutes and 46 seconds on average. All images were saved in the digital imaging and communication in medicine (DICOM) format and then reviewed by a fellowship-trained orthopedic shoulder and elbow surgeon (PNC) to ensure there was no visible shoulder pathology.

Measurement technique

All measurements were performed in third-party DICOM viewer analysis software (Horos, Pixmeo, Geneva, Switzerland). All humeral measurements were performed on axial images reoriented into the axial plane of the humerus, with both the coronal and sagittal planes parallel to a line down the center of the shaft, the origin defined as the point closest to the center of the head while still intersecting with the center of the shaft, and a line from the center of the head to the deepest point of the biceps groove defining anterior (Fig. 2). We then made measures at locations 5, 10, and 15 cm distal to the top of the head along this shaft center

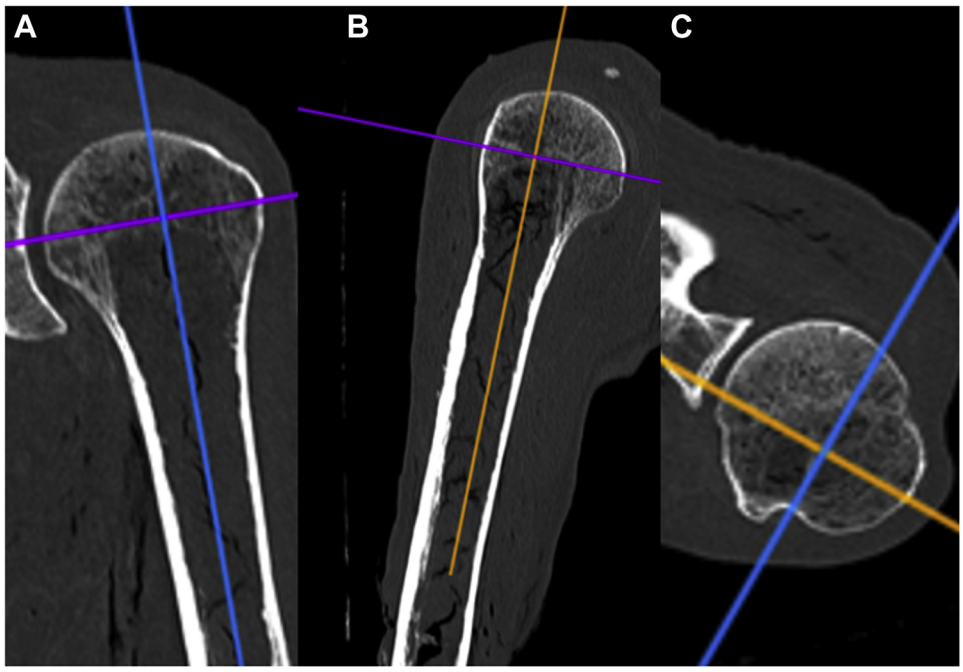

Figure 2 These computed tomographic coronal (**A**, orange line), sagittal (**B**, blue line), and axial (**C**, purple line) images demonstrate the planes for reorienting the axes to match the *Center* of the shaft, with anterior defined as a line from the *Center* of the head to the deepest point of the biceps groove (**C**).

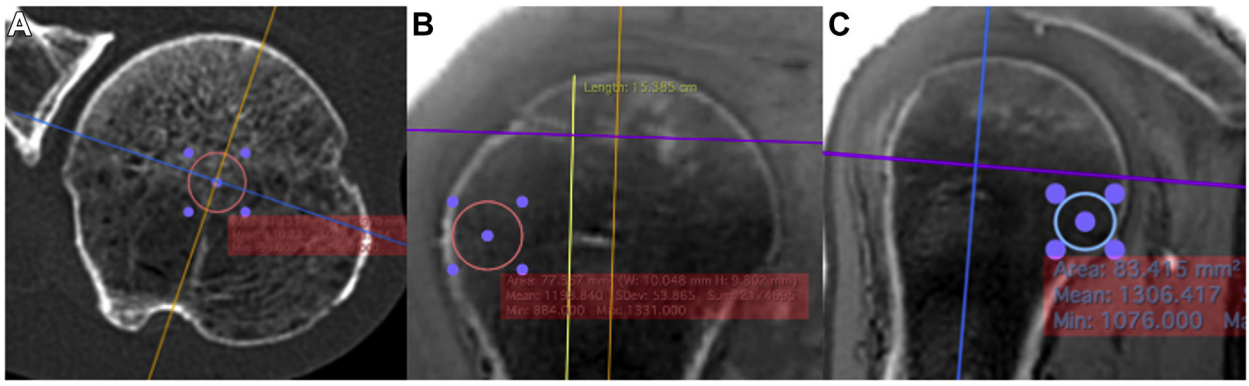

Figure 3 These ultrashort echo time magnetic resonance imaging (UTE MRI) images demonstrate the position of the 1-cm diameter region of interest (ROI) for the *Center* of the head (**A**, axial image), the subtuberosity region (**B**, coronal image), and the subarticular region (**C**, sagittal image).

line, and at each distance, we measured the maximum humeral cortical thickness at each axis (medial, lateral, anterior, posterior). To quantify cancellous density, we created circular regions of interest (ROIs) 1 cm in diameter, with the mean signal within each ROI representing cancellous density in that ROI. These ROIs were placed in the center of the head (as defined previously), just subcortical at the lateral most extent of the tuberosity on the coronal view, and just subcortical at the medial most portion of the head on the sagittal image (Fig. 3). In addition, a similar technique was used to measure ROI signal within the posterior deltoid, and all cancellous density measurements were normalized to muscle measurements, as previously described.[25]

For glenoid measurements, the axes were oriented into the plane of the glenoid by moving the origin to the center of the best-fit circle of the bottom of the glenoid and then adjusting the coronal and axial images so that the sagittal plane was parallel to a line that intersects the anterior and posterior and superior and inferior rims (Fig. 4). On the axial image, we measured the thickness of the cortex immediately medial to the center of the best-fit circle of the bottom of the glenoid. On the same axial image, we created a 1-cm diameter ROI just subcortical within the glenoid vault to measure cancellous density, which was normalized as described previously.

Statistical methods

At each distance from the top of the head, the anterior, posterior, medial, and lateral cortical thickness measurements were used to calculate a mean cortical thickness for each imaging modality and specimen. We compared cortical measurements using intraclass correlation coefficients (ICCs) with a 2-way mixed average measure for absolute agreement. In addition, we compared cortical measurements using mean differences and 95% confidence intervals for these differences, using paired Student's t-tests. We compared cancellous measurements using Pearson's correlation coefficients

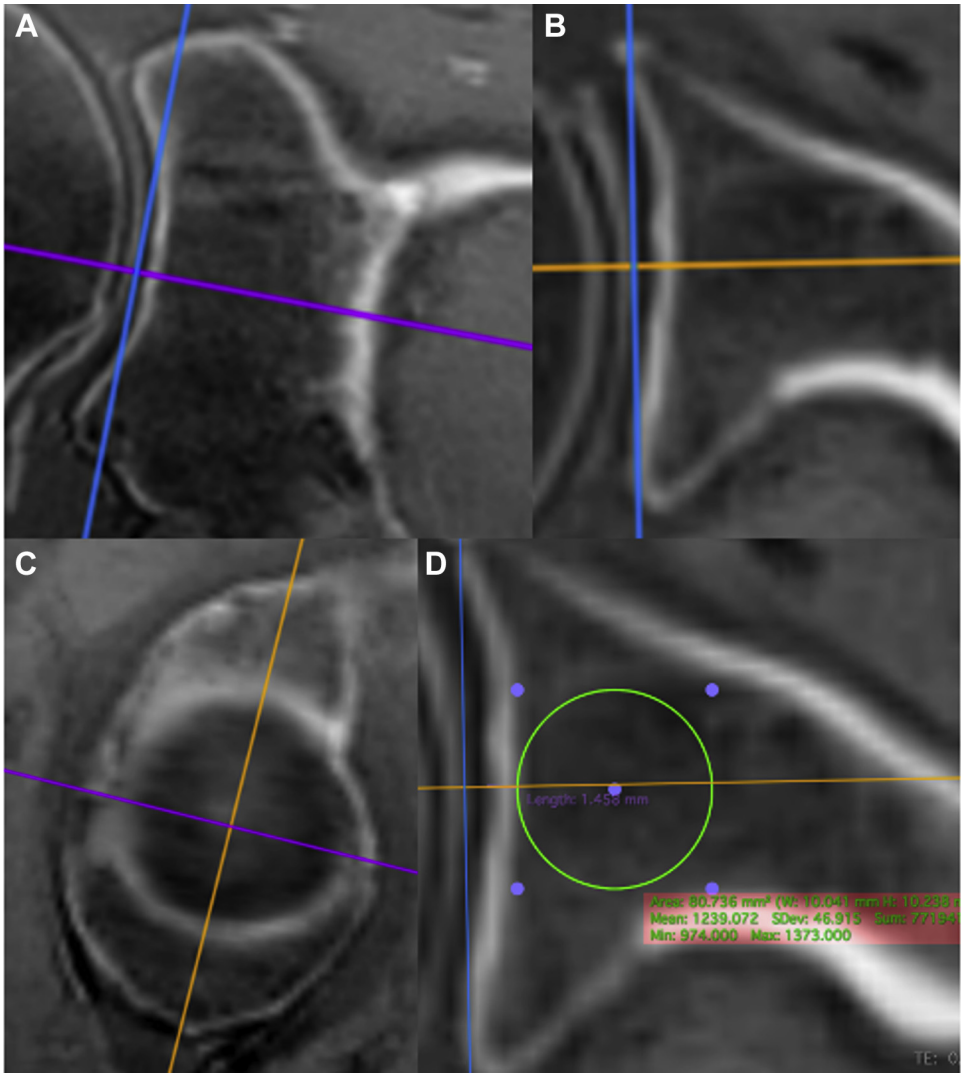

Figure 4 These ultrashort echo time magnetic resonance imaging (UTE MRI) coronal (**A**), axial (**B**), and sagittal (**C**) images demonstrate the process for reorienting the axes to match the plane of the glenoid, as defined by the *Center* of the best-fit circle (**D**) and a line parallel to a line from the anterior to the posterior rim (**B**) and a line parallel to a line from the superior to the inferior rim (**A**). Image D demonstrates the position of the 1-cm diameter region of interest for the glenoid vault (axial image).

Table I
Cortical thickness measurements for both imaging modalities.

Variable	MRI (mm)	CT (mm)	Difference (mm)	*P* value	ICC
Humerus 5 cm	2.1 [1.8 to 2.3]	2.3 [2.1 to 2.6]	0.2 [−0.2 to 0.6]	.727	0.92 [0.62 to 0.98]
Humerus 10 cm	3.2 [2.9 to 3.5]	3.6 [3.3 to 3.9]	0.4 [0.0 to 0.9]	.609	0.79 [0.08 to 0.95]
Humerus 15 cm	3.9 [3.4 to 4.4]	4.2 [3.7 to 4.7]	0.3 [−0.5 to 1.1]	.766	0.92 [0.58 to 0.98]
Glenoid	1.2 [1.0 to 1.3]	1.0 [0.9 to 1.1]	−0.2 [−0.4 to 0.0]	.255	0.48 [−1.29 to 0.88]

All data are presented as mean [95% confidence intervals]. *P* values are the results of paired Student's t tests.
MRI, magnetic resonance imaging; *CT*, computed tomography; *ICC*, intraclass correlation coefficient.

and created Bland-Altman plots for the cortical measurements.[3] All images were interpreted by two observers blinded to each other's measurements and one observer twice separated by a period of 4 weeks. Interobserver reliability and intraobserver reliability were calculated using ICCs with a 2-way mixed model for absolute agreement and average or single measurements as appropriate. We conducted all analyses in Excel (version 16, Microsoft, Redmond, WA, USA) and SPSS (version 26, IBM, Armonk, NY, USA). *A priori* we selected 0.05 as our threshold for significance and 0.75 as our lower limit for acceptability for ICCs.

Results

Cohort characteristics

We included 9 shoulders on the right side from 7 male and 2 female cadavers with a mean age at the time of death of 69 years (range, 59-80 years). The mean ± standard deviations of their height and weight were 172.2 ± 5.6 cm and 66.1 ± 23.5 kg, respectively. Cortical thickness increased with distance from the head, from a mean (95% confidence interval) of 2.3 (2.1 to 2.6) mm

Table II
Cancellous signal measurements for both imaging modalities.

Variable	MRI	CT	Correlation	*P* value
Center of the head	1.18 [1.10 to 1.26]	106 [51 to 160]	−0.087	.823
Subtuberosity	1.15 [1.04 to 1.26]	91 [66 to 116]	−0.511	.160
Subarticular	1.20 [1.08 to 1.33]	171 [141 to 200]	−0.491	.179
Glenoid vault	1.16 [1.05 to 1.27]	259 [222 to 296]	0.188	.629

All data are presented as mean [95% confidence intervals]. *P* values are the results of Pearson's correlation coefficients.
MRI data are presented as the ratio of osseous to muscle signal intensity, and CT data are presented in Hounsfield's Units.
MRI, magnetic resonance imaging; *CT*, computed tomography; *ICC*, intraclass correlation coefficient.

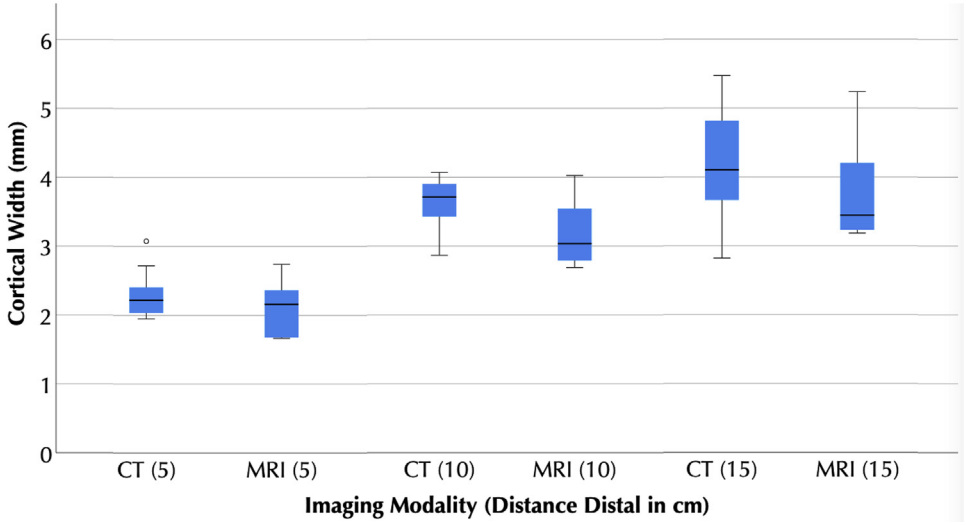

Figure 5 Box plots of computed tomography (CT) and magnetic resonance imaging (MRI) measurements of humeral cortical thickness at varying distances distal to the *Top* of the head of the humerus. No statistically significant differences were observed between modalities. The boxes represent the interquartile range, with the central line representing the median. The whiskers represent the furthest nonoutlier, nonextreme value. The dot represents an outlier.

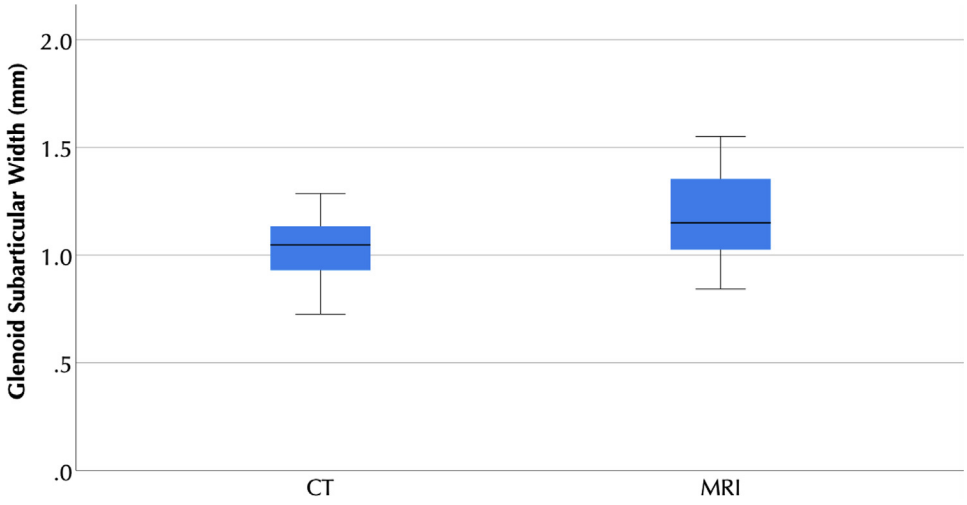

Figure 6 Box plots of computed tomography (CT) and magnetic resonance imaging (MRI) measurements of glenoid cortical thickness at the *Center* of the glenoid. No statistically significant difference was detected between modalities. The boxes represent the interquartile range, with the central line representing the median. The whiskers represent the furthest nonoutlier, nonextreme value.

at 5 cm distal to the head on CT to 4.2 (3.7 to 4.7) mm at 15 cm distal to the head. On CT, glenoid subchondral cortical thickness was 1 (0.9 to 1.1) mm at the center of the glenoid. On CT, cancellous signal was lowest in the subtuberosity region and the center of the head and highest in the subarticular region and glenoid vault (Table II).

Accuracy: UTE MRI vs. CT

For cortical thickness measurements, in all cases, the 95% confidence intervals of mean difference between MRI and CT measures included 0, and there was no statistically significant difference between measures made between modalities (Table I, Figs. 5–7).

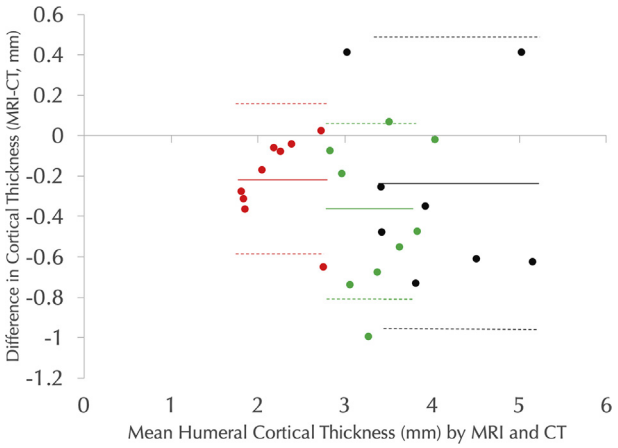

Figure 7 The Bland-Altman plot showing differences between magnetic resonance imaging (MRI) and computed tomography (CT) cortical width measurements at 5 cm distal to the *Top* of the head (red), 10 cm distal to the *Top* of the head (green), and 15 cm distal to the *Top* of the head (black). For each subpopulation, mean differences are noted by solid lines, and the 95% confidence intervals of the mean difference are shown by dotted lines.

For humeral cortical thickness measurements at all three distances from the top of the head, the ICCs were >0.75. In combination, these results suggest that UTE MRI and CT measures of humeral cortical thickness are equivalent. However, the ICCs for glenoid subchondral thickness were <0.75, suggesting that UTE MRI and CT do not reliably provide the same measurements. There was no statistically significant correlation between cancellous signal on MRI and on CT in any region, suggesting that UTE MRI cannot be used to determine cancellous density (Table II).

Reliability

For both MRI and CT, interobserver and intraobserver reliability was acceptable (ie, >0.75) for all humeral cortical thickness measures and cancellous density measures, with the exception of the interobserver reliability of the humeral subarticular region on MRI, and glenoid subchondral thickness measures did not have acceptable interobserver or intraobserver reliability on either MRI or CT (Table III).

Discussion

The purpose of this study was to determine whether UTE MRI could accurately and reliably quantify proximal humeral cortical thickness, subchondral glenoid thickness, and cancellous density as compared with CT. The UTE MRI was able to accurately measure proximal humeral cortical thickness, as no statistically significant difference between modalities was detected and the comparative ICCs were >0.75. In addition, on both CT and UTE MRI, proximal humeral cortical thickness has acceptable (>0.75) ICCs for both inter-rater and intrarater reliability. In combination, these results validate UTE MRI measures of proximal humeral cortical thickness, which is clinically relevant as proximal humeral cortical thickness correlates with bone mineral density and can thus be used to rule out osteoporosis.[23] However, UTE MRI cannot be used to accurately measure cancellous density as these measures did not correlate with CT measures for any of the regions measured. In addition, neither UTE MRI nor CT can accurately or reliably measure glenoid cortical thickness.

Our results suggest that UTE MRI can reliably delineate proximal humeral cortical thickness. Prior research is conflicting on the ability of MRI to delineate cortical anatomy. For instance, several studies have examined use of standard MRI sequences to measure glenoid bone loss in the setting of glenohumeral instability, with differing results.[2,10,11,19,22,29,35,39] Within the present study, glenoid cortical thickness could not be accurately measured, likely because the glenoid articular cortical thickness is only 1.1 mm. However, several studies have demonstrated MRI to be capable for accurately measuring long bone cortical thickness.[7,27,28] In concert with our own findings, these suggest that UTE MRI is an accurate and reliable method for measuring proximal humeral cortical thickness.

With our methods, UTE MRI had acceptable interobserver and intraobserver reliability for cancellous density but did not significantly correlate with CT measures. Multiple prior studies have examined MRI's ability to determine trabecular bone quality, with mixed results. For instance, a prior study demonstrated MRI measures to be the worst correlate with screw fixation strength in the vertebral body, when compared with DEXA and CT.[8] Multiple recent studies have examined more complex methodologies, such as examination of trabecular morphology using the surface-to-curve ratio[31,32,36] and direct measurements of trabecular number and thickness.[12] Our results suggest that it will be necessary to apply these more computationally intensive and/or experimental methodologies for MRI to accurately measure cancellous bone quality.

This study has several limitations. As this was a cadaver study, these scans were performed under ideal conditions. Specifically, with cadavers there is no motion artifact to degrade MRI images, and high-density image quality was achieved as there were no time or radiation limitations to consider. As these were isolated cadaveric shoulder specimens, we are not able to determine whether UTE MRI humeral cortical thickness measurements correlate with traditional clinical DEXA measurements of the femoral neck and lumbar spine. This study also had a small sample size, but benefitted from the strength of a repeated measure study design.

Table III
Reliability statistics.

Variable	Interobserver		Intraobserver	
	MRI	CT	MRI	CT
Humerus 5 cm	**0.753 [−0.094 to 0.944]**	**0.886 [0.494 to 0.974]**	**0.898 [0.549 to 0.977]**	**0.968 [0.860 to 0.993]**
Humerus 10 cm	**0.799 [0.110 to 0.955]**	**0.847 [0.322 to 0.966]**	**0.775 [0.002 to 0.949]**	**0.928 [0.681 to 0.984]**
Humerus 15 cm	**0.991 [0.962 to 0.998]**	**0.761 [−0.059 to 0.946]**	**0.900 [0.500 to 0.980]**	**0.983 [0.924 to 0.996]**
Glenoid	−0.362 [−0.809 to 0.350]	0.017 [−0.621 to 0.642]	−0.373 [−0.813 to 0.339]	0.425 [−0.283 to 0.833]
Center of the head	**0.954 [0.812 to 0.990]**	**0.900 [0.623 to 0.977]**	**0.987 [0.944 to 0.997]**	**0.948 [0.789 to 0.988]**
Subtuberosity	**0.932 [0.731 to 0.984]**	**0.895 [0.607 to 0.975]**	**0.952 [0.804 to 0.989]**	**0.841 [0.445 to 0.962]**
Subarticular	0.575 [−0.089 to 0.885]	**0.853 [0.480 to 0.965]**	**0.975 [0.895 to 0.994]**	**0.908 [0.647 to 0.978]**
Glenoid vault	**0.989 [0.954 to 0.998]**	**0.912 [0.660 to 0.979]**	**0.987 [0.943 to 0.997]**	**0.955 [0.813 to 0.990]**

All values represent intraclass correlation coefficients [95% confidence intervals]. Acceptable values, that is >0.75, are bolded.
MRI, magnetic resonance imaging; *CT*, computed tomography.

These scans were of normal cadavers, and thus, our results may not be generalizable to shoulders with glenohumeral osteoarthritis, rotator cuff tears, or glenohumeral instability. Both observers included in this study have extensive experience using the measurement techniques described herein, as similar techniques have been used in prior studies. However, these results are sufficiently promising to proceed with inclusion of the UTE pulse sequence within several of our clinical scan protocols, facilitating future research to confirm the accuracy and reliability of these results. Finally, for UTE MRI to fully replace CT in imaging for shoulder surgery, it will need to provide three-dimensional auto-segmentations sufficiently accurate for prearthroplasty planning software. Further studies will be necessary to assess UTE MRI's capabilities in this regard.

Conclusion

UTE MRI can be used to reliably and accurately measure humeral cortical thickness, but cannot accurately measure cancellous density or glenoid cortical thickness.

Disclaimers:

Funding: The research reported in this publication was supported by the National Institute of Arthritis and Musculoskeletal and Skin Diseases (NIAMS) of the National Institutes of Health under award number R01 AR067196, and a Shared Instrumentation Grant S10 OD021644. The research content herein is solely the responsibility of the authors and does not necessarily represent the official views of the National Institutes of Health.

Conflicts of interest: Garrett Christensen, Hiroaki Ishikawa, Heath Henninger, Eugene Kholmovski, and Megan Mills certify that they have no commercial associations (eg, consultancies, stock ownership, equity interest, patent/licensing arrangements, etc.) that might pose a conflict of interest in connection with the submitted article. Robert Tashjian is a paid consultant for Zimmer and Mitek; has stock in CoNextions, Intrafuse, and KATOR; receives intellectual property royalties from Shoulder Innovations, Wright Medical, and Zimmer; receives publishing royalties from the Journal of Bone and Joint Surgery; and serves on the editorial board for the Journal of Orthopaedic Trauma. Peter Chalmers is a paid consultant for Depuy and DJO, is a paid speaker for Depuy, receives royalties from Depuy, and serves on the editorial board for the Journal of Shoulder and Elbow Surgery.

References

1. Akkawi I, Zmerly H. Osteoporosis: current Concepts. Joints 2018;06:122-7. https://doi.org/10.1055/s-0038-1660790.
2. Bishop JY, Jones GL, Rerko MA, Donaldson C, Group MS. 3-D CT is the most reliable imaging modality when quantifying glenoid bone loss. Clin Orthop Relat Res 2013;471:1251-6. https://doi.org/10.1007/s11999-012-2607-x.
3. Bland JM, Altman DG. Statistical methods for assessing agreement between two methods of clinical measurement. Lancet 1986;1:307-10.
4. Cancienne JM, Brockmeier SF, Kew ME, Deasey MJ, Werner BC. The association of osteoporosis and Bisphosphonate Use with Revision shoulder surgery after rotator cuff repair. Arthrosc J Arthrosc Relat Surg 2019;35:2314-20. https://doi.org/10.1016/j.arthro.2019.03.036.
5. Casp AJ, Montgomery SR, Cancienne JM, Brockmeier SF, Werner BC. Osteoporosis and Implant-Related complications after anatomic and Reverse Total shoulder arthroplasty. J Am Acad Orthop Sur 2019;1. https://doi.org/10.5435/jaaos-d-18-00537.
6. Chalmers PN, Christensen G, O'Neill D, Tashjian RZ. Does bone loss imaging modality, measurement methodology, and Interobserver reliability Alter treatment in glenohumeral instability? Arthrosc J Arthrosc Relat Surg 2020;36:12-9. https://doi.org/10.1016/j.arthro.2019.06.025.
7. Chen H, Sprengers AMJ, Kang Y, Verdonschot N. Automated segmentation of trabecular and cortical bone from proton density weighted MRI of the knee. Med Biol Eng Comput 2019;57:1015-27. https://doi.org/10.1007/s11517-018-1936-7.
8. Eysel P, Schwitalle M, Oberstein A, Rompe JD, Hopf C, Küllmer K. Preoperative Estimation of screw fixation strength in vertebral Bodies. Spine 1998;23:174-80.
9. Fitzgerald M, Lawler SM, Lowe JT, Nelson R, Mantell MT, Jawa A. Computed tomography underestimates rotator cuff pathology in patients with glenohumeral osteoarthritis. J Shoulder Elbow Surg 2018;27. https://doi.org/10.1016/j.jse.2018.02.034.
10. Gyftopoulos S, Hasan S, Bencardino J, Mayo J, Nayyar S, Babb J, et al. Diagnostic accuracy of MRI in the measurement of glenoid bone loss. Am J Roentgenol 2012;199:873-8. https://doi.org/10.2214/ajr.11.7639.
11. Huijsmans PE, Haen PS, Kidd M, Dhert WJ, van der Hulst VPM, Willems WJ. Quantification of a glenoid defect with three-dimensional computed tomography and magnetic resonance imaging: a cadaveric study. J Shoulder Elbow Surg 2007;16:803-9. https://doi.org/10.1016/j.jse.2007.02.115.
12. Issever AS, Link TM, Newitt D, Munoz T, Majumdar S. Interrelationships between 3-T-MRI-derived cortical and trabecular bone structure parameters and quantitative-computed-tomography-derivedbone mineral density. Magn Reson Imaging 2010;28:1299-305. https://doi.org/10.1016/j.mri.2010.06.003.
13. Jerban S, Lu X, Jang H, Ma Y, Namiranian B, Le N, et al. Significant correlations between human cortical bone mineral density and quantitative susceptibility mapping (QSM) obtained with 3D Cones ultrashort echo time magnetic resonance imaging (UTE-MRI). Magn Reson Imaging 2019;62:104-10. https://doi.org/10.1016/j.mri.2019.06.016.
14. Jonas SC, Walton MJ, Sarangi PP. Is MRA an unnecessary expense in the management of a clinically unstable shoulder? Acta Orthop 2012;83:267-70. https://doi.org/10.3109/17453674.2012.672090.
15. Kawakami J, Yamamoto N, Nagamoto H, Itoi E. Minimum distance of Suture Anchors used for rotator cuff repair without Decreasing the Pullout strength: a Biomechanical study. Arthrosc J Arthrosc Relat Surg 2017;34. https://doi.org/10.1016/j.arthro.2017.07.022.
16. Kim JY, Park JS, Rhee YG. Can preoperative magnetic resonance imaging Predict the Reparability of Massive rotator cuff tears? Am J Sports Med 2017;45:1654-63. https://doi.org/10.1177/0363546517694160.
17. Kim SH, Szabo RM, Marder RA. Epidemiology of humerus fractures in the United States: nationwide emergency department sample, 2008. Arthrit Care Res 2012;64:407-14. https://doi.org/10.1002/acr.21563.
18. Lansdown DA, Cvetanovich GL, Verma NN, Cole BJ, Bach BR, Nicholson G, et al. Automated 3-dimensional magnetic resonance imaging allows for accurate evaluation of glenoid bone loss compared with 3-dimensional computed tomography. Arthrosc J Arthrosc Relat Surg 2019;35:734-40. https://doi.org/10.1016/j.arthro.2018.10.119.
19. Lee RKL, Griffith JF, Tong MMP, Sharma N, Yung P. Glenoid bone loss: assessment with MR imaging. Radiology 2013;267:496-502. https://doi.org/10.1148/radiol.12121681.
20. Link T, Heilmeier U. Bone quality—beyond bone mineral density. Semin Musculoskel R 2016;20:269-78. https://doi.org/10.1055/s-0036-1592365.
21. Maier D, Jaeger M, Izadpanah K, Strohm PC, Suedkamp NP. Proximal humeral fracture treatment in adults. J Bone Jt Surg 2014;96:251-61. https://doi.org/10.2106/jbjs.l.01293.
22. Markenstein JE, Jaspars KCJ, van der Hulst VPM, Willems WJ. The quantification of glenoid bone loss in anterior shoulder instability; MR-arthro compared to 3D-CT. Skeletal Radiol 2014;43:475-83. https://doi.org/10.1007/s00256-013-1780-7.
23. Mather J, MacDermid JC, Faber KJ, Athwal GS. Proximal humerus cortical bone thickness correlates with bone mineral density and can clinically rule out osteoporosis. J Shoulder Elbow Surg 2013;22:732-8. https://doi.org/10.1016/j.jse.2012.08.018.
24. McCarthy JC. The diagnosis and treatment of labral and chondral injuries. Instructional Course Lectures 2004;53:573-7.
25. McKee TC, Dave J, Kania L, Karajgikar J, Masarapu V, Deshmukh S, et al. Are Hemorrhagic Cysts Hyperintense Enough on T1-weighted MRI to Be Distinguished from Renal Cell Carcinomas? A Retrospective analysis of 204 patients. Am J Roentgenol 2019;213:1267-73. https://doi.org/10.2214/ajr.19.21257.
26. Östör AJK, Richards CA, Tytherleigh-Strong G, Bearcroft PW, Prevost AT, Speed CA, et al. Validation of clinical examination versus magnetic resonance imaging and arthroscopy for the detection of rotator cuff lesions. Clin Rheumatol 2013;32:1283-91. https://doi.org/10.1007/s10067-013-2260-0.
27. Preidler KW, Brossmann J, Daenen B, Pedowitz R, Maeseneer MD, Trudell D, et al. Measurements of cortical thickness in experimentally created endosteal bone lesions: a comparison of radiography, CT, MR imaging, and anatomic sections. Am J Roentgenol 1997;168:1501-5.
28. Ramme AJ, Vira S, Hotca A, Miller R, Welbeck A, Honig S, et al. A Novel MRI Tool for evaluating cortical bone thickness of the proximal Femur. Bull Hosp Jt Dis 2013 2019;77:115-21.
29. Rerko MA, Pan X, Donaldson C, Jones GL, Bishop JY. Comparison of various imaging techniques to quantify glenoid bone loss in shoulder instability. J Shoulder Elbow Surg 2013;22:528-34. https://doi.org/10.1016/j.jse.2012.05.034.
30. Reuther F, Mühlhäusler B, Wahl D, Nijs S. Functional outcome of shoulder hemiarthroplasty for fractures: a multicentre analysis. Inj 2010;41:606-12. https://doi.org/10.1016/j.injury.2009.11.019.
31. Sharma AK, Toussaint ND, Elder GJ, Masterson R, Holt SG, Robertson PL, et al. Magnetic resonance imaging based assessment of bone microstructure as a non-invasive alternative to histomorphometry in patients with chronic kidney

disease. Bone 2018;114:14-21. https://doi.org/10.1016/j.bone.2018.05.029.
32. Sharma AK, Toussaint ND, Elder GJ, Rajapakse CS, Holt SG, Baldock P, et al. Changes in bone microarchitecture following kidney transplantation—beyond bone mineral density. Clin Transpl 2018;32:e13347. https://doi.org/10.1111/ctr.13347.
33. Smark CT, Barlow BT, Vachon TA, Provencher MT. Arthroscopic and magnetic resonance arthrogram features of Kim's lesion in posterior shoulder instability. Arthrosc J Arthrosc Relat Surg 2014;30:781-4. https://doi.org/10.1016/j.arthro.2014.02.038.
34. Sollmann N, Löffler MT, Kronthaler S, Böhm C, Dieckmeyer M, Ruschke S, et al. MRI-Based quantitative osteoporosis imaging at the spine and Femur. J Magn Reson Imaging 2020. https://doi.org/10.1002/jmri.27260.
35. Stecco A, Guenzi E, Cascone T, Fabbiano F, Fornara P, Oronzo P, et al. MRI can assess glenoid bone loss after shoulder luxation: inter- and intra-individual comparison with CT. La Radiologia Med 2013;118:1335-43. https://doi.org/10.1007/s11547-013-0927-x.
36. Wehrli FW, Ladinsky GA, Jones C, Benito M, Magland J, Vasilic B, et al. In Vivo magnetic resonance Detects Rapid Remodeling Changes in the Topology of the trabecular bone Network after Menopause and the Protective Effect of Estradiol. J Bone Miner Res 2008;23:730-40. https://doi.org/10.1359/jbmr.080108.
37. Werthel J-D, Schoch BS, van Veen SC, Elhassan BT, An K-N, Cofield RH, et al. Acromial fractures in Reverse shoulder arthroplasty: a clinical and radiographic analysis. J Shoulder Elbow Arthroplast 2018;2:2471549218777628. https://doi.org/10.1177/2471549218777628.
38. Xie Y, Liu S, Qu J, Wu P, Tao H, Chen S. Quantitative magnetic resonance imaging UTE-T2* mapping of tendon Healing after arthroscopic rotator cuff repair: a Longitudinal study. Am J Sports Med 2020:036354652094677. https://doi.org/10.1177/0363546520946772.
39. Yanke AB, Shin JJ, Pearson I, Bach BR, Romeo AA, Cole BJ, et al. Three-dimensional magnetic resonance imaging quantification of glenoid bone loss is equivalent to 3-dimensional computed tomography quantification: cadaveric study. Arthrosc J Arthrosc Relat Surg 2017;33:709-15. https://doi.org/10.1016/j.arthro.2016.08.025.